Available online at www.sciencedirect.com
SCIENCE DIRECT
ELSEVIER
Colloids and Surfaces A: Physicochem. Eng. Aspects xxx (2006) xxx–xxx
COLLOIDS AND SURFACES A
www.elsevier.com/locate/colsurfa

The formation and stability of self-assembled monolayers of octadecylphosphonic acid on titania

A. Kanta, R. Sedev, J. Ralston *

Ian Wark Research Institute, University of South Australia, Mawson Lakes, Adelaide, SA 5095, Australia

Received 11 August 2005; received in revised form 12 December 2005; accepted 26 December 2005

Abstract

Octadecylphosphonic acid (OPA) forms monolayers on amorphous smooth titania surfaces. The OPA was deposited by immersion in tetrahydrofuran solutions. The process takes place rapidly at 2×10^{-4} M OPA, evidence of which is an advancing water contact angle of approx. 100° after 10 s of immersion. The advancing water contact angle plateaus at $110 \pm 2°$ after several hours. At lower concentrations (2×10^{-6} and 2×10^{-8} M OPA), only partial coverage of OPA on titania films is achieved.

OPA self-assembled monolayers (SAMs) are resistant to exposure to common solvents. Water wettability is a function of the molecular volume of the solvents. Whereas low molecular volume liquids penetrate OPA SAMs, no penetration is observed for high molecular volume liquids. The cross-sectional area of pores in the OPA monolayers is estimated at 27 Å^2.

UV light ($\lambda = 250$ nm), heat treatment and air plasma all significantly improve the wettability of OPA SAMs, resulting in a water contact angle of 0°. The presence of phosphorus shows that the bond of the phosphate headgroup to titania through oxygen atom(s) is strong and can withstand these conditions.

Keywords: Octadecylphosphonic acid; Titania; Self-assembled monolayers; Wettability; Contact angle

1. Introduction

Self-assembled monolayers (SAMs) are molecular assemblies formed spontaneously by the immersion of a substrate into a solution of the active surfactant [1]. SAMs have attracted widespread and growing interest, since they provide a versatile tool for surface modification in a wide range of technologies, e.g. corrosion resistance, biosensors, microelectronics and catalysis. They also serve as excellent model systems for evaluating theories of wetting, adhesion, friction and related phenomena [1]. A vast majority of SAMs studies until now have been focused on the interactions of chlorosilanes with OH-terminated oxide surfaces [2] and on the adsorption of thiols on gold [3]. Potential applications of alkyltrichlorosilane SAMs in the engineering of surface properties are somewhat limited due to the polymeric nature of these assemblies [1]. Alkanethiols usually form SAMs with a higher degree of perfection. The use of gold as a substrate, however, may pose a problem in applications where optical transparency is an issue. Furthermore, gold is not a suitable material for silicon processing in microelectronics. A small number of studies employ alternative chemistries, e.g. carboxylic acid [4], phosphoric acid [5] and phosphonic acids [6]. Films of alkanephosphonic acids assemble on the surface, probably through hydrogen-bonding between phosphonic acid headgroups as well as van der Waals interactions between adjacent methylene units [7]. Octadecylphosphonic acid ($CH_3(CH_2)_{17}PO_3H_2$, OPA) is a typical example. Gawalt et al. [6,7] investigated the adsorption of alkanephosphonic acids on the native oxide surface of titanium. Both titania and the native oxide layer of titanium foil were found to be rather unreactive toward alkanephosphonic acids at room temperature, and a surface modification reagent was used to attach the acid to the metal oxide substrate [6]. This relative inertness was verified in the NMR studies of Gao [8], who found that phosphonic acids react strongly with ZrO_2, however, the analogous reaction with titania was poor. Vibrational spectroscopy and AFM imaging results suggest that OPA is weakly held on a titania surface [7], that the chains are ordered in island-like structures [8] or that formation takes place via a uniformly

* Corresponding author. Tel.: +61 8 8302 3066; fax: +61 8 8302 3683.
E-mail address: john.ralston@unisa.edu.au (J. Ralston).

0927-7757/$ – see front matter © 2006 Elsevier B.V. All rights reserved.
doi:10.1016/j.colsurfa.2005.12.057

disordered monolayer, which, beyond a surface coverage of 50% gradually becomes ordered [9]. There is no consensus regarding the mechanism of formation.

For mica the situation is rather different [10–14]. OPA spontaneously self-assembles onto mica in the form of irregular islands distributed randomly over the surface. The coverage of the mica surface can be varied by altering the concentration of the OPA solution and the immersion time [15,16]. Regardless of the duration of the adsorption, the height of the OPA islands was reported [16] to be 1.8 ± 0.2 nm, suggesting a tilt angle of about 40° [16] or, alternatively, a degree of disorder in the hydrocarbon chain. The maximum value of the advancing water contact angle obtained on OPA monolayers on the mica surface after 2 h of adsorption was 89° [16], i.e. approximately 20° less than expected for water on well-ordered methyl-terminated surface [17]. Moreover, the slow spreading of water droplet when contacting the OPA/mica surface, together with a significant decrease in water contact angle (from 90° to 55°) following sonication in water, as well as inconsistent values for the receding contact angles [16] are all indicative of surface damage due to exposure to water. These various studies suggest that there is considerable chain disorder in OPA SAMs on mica.

OPA also forms SAMs on common engineering metals, such as steel, copper and brass [18]. Adsorption of phosphonic acids and phosphates occurs on several transition metal oxides, e.g. Ta_2O_5, Al_2O_3, Nb_2O_5, ZrO_2 and also on zircon [19–21]. Phosphates do not form SAM on silica due to a much lower affinity of phosphate for Si(IV) in comparison to Ti(IV), Al(IV), Nb(IV) or Ta(V), which form metal–cation coordination bonds [19].

The present work investigates the formation of OPA SAMs on amorphous smooth thin films of titania and their stability. Particular emphasis is placed upon exposure to various solvents, so as to investigate the stability of the OPA monolayers. The influence of UV light irradiation, heat treatment and air plasma were assessed. Tapping Mode Atomic force microscopy, contact angle determinations and surface spectroscopy were used as investigative tools.

2. Experimental

The synthesis of octadecylphosphonic acid was carried out as follows [22]. 1-Octadecene (50 g) was refluxed with phosphonic acid (50 g) at ~110 °C for 8 h in the presence of benzoyl peroxide (5 g). All materials were obtained from Aldrich and were used without further purification. The solvent used was 1,4-dioxane and the reaction was carried out in a dry nitrogen atmosphere. After refluxing, the solution was cooled overnight, during which white crystals precipitated from the solution. The crystals were filtered, washed in 1,4-dioxane and recrystallised from a warm mixture of 1:1 acetone/methylethylketone (Ajax Finechem). The final product was dried in air. The product was analysed by ^{1}H NMR spectroscopy with the following results: 0.88 (t, 3 H, terminal $–CH_3–$), 1.25 (m, 34 H, long chain $–(CH_2)_{17}–$), 1.65 (broad s, 2 H, $–PO_3H_2$), fully in accordance with literature data [23].

Silicon wafers covered with a thin layer of titanium dioxide were obtained from Philips Research Laboratories (Eindhoven, The Netherlands). Magnetron sputtering was used to deposit layers of pure and stoichiometric TiO_2 (details can be found elsewhere [24]). The root-mean-square (RMS) roughness of the layers was 0.4 nm and the peak-to-valley height was 1.2 nm over an area of 1 μm^2.

All solvents used for the investigation of stability of OPA SAMs were analytical reagents and were used as received. They were obtained from Ajax Finechem (methanol, ethanol and acetone) and Chem-Supply (cyclohexane and toluene). Tetrahydrofuran (laboratory reagent) was obtained from Chem-Supply and used as received.

Prior to deposition, titania substrates were cleaned as follows: they were thoroughly rinsed with high-purity water and ethanol, sonicated in ethanol for 10 min, rinsed with copious amounts of high-purity water and blown dry with filtered nitrogen. Finally, they were plasma-cleaned for 60 s. This treatment resulted in a completely hydrophilic surface (water contact angle of 0°). Immersion of clean titania wafers in OPA/THF solution was carried out immediately after the cleaning because of the extreme susceptibility of these titania films to adventitious hydrocarbon contamination [25]. Self-assembled monolayers of OPA were prepared by immersion of clean titania substrates in solutions of OPA in THF. Upon removal the samples were rinsed in pure THF for 30 s and finally blown dry with filtered nitrogen.

Surface imaging was performed with an atomic force microscope (NanoScope III, Digital Instruments) in tapping mode. Silicon cantilevers (NT-MDT, spring constant of 11.5 N m^{-1}) were used to collect detailed topographic information. RMS roughness and peak-to-valley height were obtained with the AFM running software (NanoScope® IIIa, version 5.12b42, Digital Instruments). AFM was regularly calibrated with a silicon grid (3D reference, Digital Instruments).

Advancing water contact angles were measured using the sessile drop method. Digital images of the droplet silhouette (624 pixels × 580 pixels, 256 grey levels) were captured with a progressive scan CCD camera (JAI CV-M10BX). The contact angle was determined by numerically drawing a tangent close to the edge of the droplet. All measurements were performed with high-purity water at pH 5.8 (resistivity >18 MΩ cm and surface tension of 72.8 mN/m at 20 °C). The wettability data presented are an average of at least 10 measurements. In the investigation of the OPA stability upon solvent exposure, three independent experiments (at least 10 contact angle measurements each) were carried out.

The samples used to investigate the solvent influence were treated as follows. They were immersed in the specified solvent for 18 h at room temperature, removed with a clean pair of tweezers, rinsed for 10 s with Milli-Q water and blown dry (5 s) with filtered nitrogen gas.

X-ray photoelectron spectroscopy (XPS) analyses were performed using a Physical Electronics PHI Model 5600 hemispheric electron spectrometer, employing a non-monochromatic Mg Kα source (1253.6 eV) operated at 300 W. The XPS was calibrated with the silver $3d_{5/2}$ and copper $2p_{3/2}$ photoelectron peaks after sputtering the silver and copper surfaces with an argon ion beam for 2 min to remove the surface contamination. A fixed pass energy of 93.9 eV for survey scans and 29.35 eV

for multiplex scans were used. All XPS measurements were acquired at a take-off angle of 45° to the surface. During analysis, the base pressure remained below 1×10^{-8} mbar. All peaks were referenced to the C(1s) (hydrocarbon C–C, C–H) contribution at 284.8 eV. Acquisition times were approx. 5 min for survey scans and 11 min for high resolution elemental scans. In the case of multiplex scans, five sweeps were used for carbon and phosphorus and three sweeps for titanium and oxygen. The XPS measurements reported here were carried out ex situ. The samples were analysed immediately after different surface treatment; the transfer of samples into the vacuum chamber took less than 1 min.

Time-of-flight secondary ion mass spectroscopy (ToF-SIMS) measurements were performed on a PHI TRIFT 2100 time-of-flight secondary ion mass spectrometer equipped with a pulsed 15 keV Ga liquid metal ion gun (LMIG). The primary ion-beam current was 600 pA, the pulse rate was 10 kHz, and the acquisition time was 60 s. To ensure that only a small fraction of surface material was removed, the primary ion current density on the sample was reduced to less than 5×10^{12} ions/cm^2 during acquisition.

Negative spectra were acquired from the OPA SAMs in the mass range m/z = 0–200. The relative intensities were used, since a matrix effect complicates quantification of results [26].

On each sample ten spots of size 100 μm × 100 μm were analysed. Each intensity ratio is expressed as an average value with a 95% confidence interval. Prior to statistical analysis, the data were normalised by dividing the intensity of the ion of interest by that of the ion yield for the sum of all peaks. The analysed materials were loaded into the SIMS chamber within 1 min in a home-made quartz cell to minimize contamination.

OPA SAMs on titania films were irradiated in ambient atmosphere (humidity 50%) with UV light of fixed wavelength (λ = 250 nm) using a spectral irradiator MM3 (Bunkoh-Keiki Co., Japan) equipped with a 2 kW Xenon lamp. The intensity of UV light was 1.0 mW/cm^2. Samples were irradiated for up to 180 min (energy of 10.4 J/cm^2 measured at the sample surface).

Thermal treatment was carried out for 6 h in air in an oven (Jetflow model K2F, Australia). Samples were placed in a custom-built quartz cell to minimize contamination.

Samples were subsequently cooled down to 100 °C (3 h), taken out of the oven and immediately analysed.

The plasma exposure was carried out in a Harrick Plasma Unit (model PDC-32G), operated at 100 W and frequency 13.56 MHz.

3. Results and discussion

3.1. Formation of OPA SAM on amorphous titania films

Fig. 1 shows changes in the advancing water contact angle on titania films as a function of immersion time in OPA (2×10^{-4} M THF solution). The contact angle increases rapidly—a value of 100° was observed after 1 min of immersion but similar values were obtained after adsorption times as short as 10 s. After the initial jump the advancing water contact angle increases gradually and plateaus at 110 ± 2° after several hours of immersion.

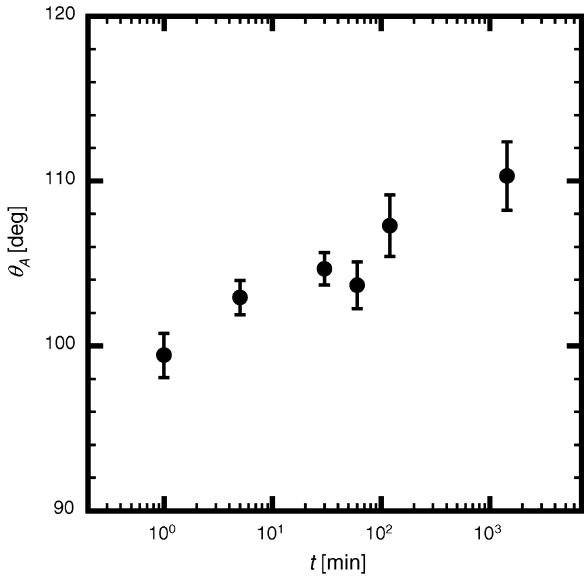

Fig. 1. Advancing contact angle of water on OPA SAMs formed on titania films as a function of the immersion time in OPA (2×10^{-4} M solution in THF).

No further increase was observed, even after several days of immersion at this concentration.

The layers of OPA molecules were rather smooth and homogeneous, as seen with AFM. RMS roughness of the titania substrate (0.4 ± 0.1 nm) did not change after adsorption of OPA molecules. AFM imaging revealed featureless topographical and phase images on surfaces after 10 s of immersion in OPA/THF. The same was found after immersion periods of up to 24 h. The absence of any islands in the phase images, in conjunction with contact angle data, confirmed the complete coverage of OPA films.

The plateau contact angle reached after several hours of immersion suggests that well-ordered, closely-packed methyl-terminated OPA monolayers are formed. The value (∼110°) reached after several hours is in accordance other studies [19].

For the sake of comparison, the adsorption of OPA onto the surface of mica (2×10^{-4} M OPA) was studied. The formation of randomly scattered OPA islands was observed. As the immersion time increased, the islands increased in size and grew together, which was supported by contact angle measurements. AFM images of OPA on mica (not shown) were similar to those published in the literature [15,16,27,28].

The formation of OPA SAMs on titania films is quite different from the formation of these SAMs on mica [16]. The formation of OPA SAMs proceeds faster on titania than on mica. Whereas short adsorption times (of the order of minutes) yield only partial coverage on mica, titania films are swiftly covered by the OPA SAMs. We note that we used the same concentration (2×10^{-4} M) as Woodward et al. [16], who observed water contact angles of ∼60° after several minutes of adsorption. Our contact angle data on titania films, however, clearly imply the presence of homogeneous OPA SAMs. The slight increase (from 100° to 110°) in the advancing water contact angles with immersion time on titania can be ascribed to a conversion of disordered alkyl chains to ordered chains during the

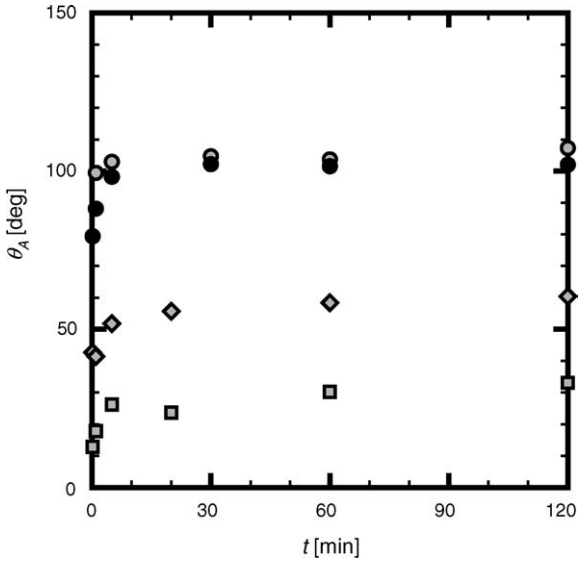

Fig. 2. Advancing contact angle of water on OPA SAMs formed on titania films as a function of the immersion time in OPA solutions in THF: (◯) 2×10^{-4} M; (◇) 2×10^{-6} M; (□) 2×10^{-8} M; and (●) 2×10^{-4} M, 2 °C.

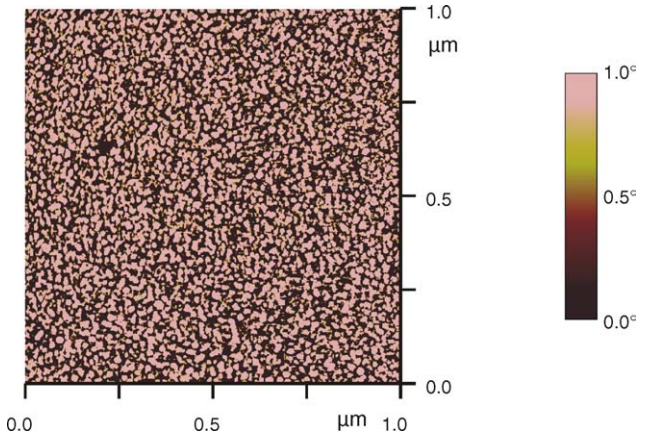

Fig. 3. Tapping mode AFM phase image of OPA SAMs formed on titania films after a 10 s immersion in 2×10^{-6} M OPA solution in THF.

film growth. The homogeneous morphology of the surface of OPA SAMs on titania films (i.e. the absence of islands) is supported by the AFM phase images where no island-like structures were observed (10 s, 2 and 24 h immersion times were tested). We note that our contact angle data are in agreement with published infrared studies [9].

The OPA SAMs formation on smooth titania films reported here is essentially the same as on sapphire [29] at room temperature: similar water contact angles were measured after short adsorption times on alumina and were accompanied by featureless topographical images. The OPA SAMs also grow as continuous, slightly disordered layers, on single crystal α-Al_2O_3 surfaces.

We also tested the adsorption of OPA on titania at lower concentrations (2×10^{-6} and 2×10^{-8} M OPA) in the same solvent. Fig. 2 shows that water contact angle increases rather slowly after immersion of titania films in these solutions, suggesting that only partial coverage is achieved. The growth is therefore expected to proceed through the formation of islands, partially covering the titania surface.

A reliable determination of the height of the OPA islands on titania was not feasible on our substrate. It has been established [7,19] that a tilt angle of approximately 30° is found in phosphate-metal oxide systems. This value corresponds to a height of approx. 2 nm, for a sufficiently smooth substrate. The AFM characterization of the titania films has been published elsewhere [25]. The biggest features observed by Messerschmidt and Schwartz [29] on OPA adsorbed on molecularly smooth alumina (a material with similar adsorption characteristics [29]) were only 0.8 nm. Such dimensions cannot be measured on our substrate (peak-to-valley height 1.2 nm); however, the presence of island-like structures of OPA molecules was ascertained by AFM phase images (Fig. 3).

Finally, we investigated the growth process of OPA on titania films at lower temperature (2 °C, 2×10^{-4} M OPA). Fig. 2 shows an increase in water contact angle after immersing titania films in 2×10^{-4} M OPA solution at room temperature and at 2 °C. It can be seen that the formation of OPA SAMs proceeds at slower rate at low temperature; this is similar to the growth of OPA SAMs on α-Al_2O_3 [29].

In our experiments, only 2×10^{-4} M OPA solution yields closely-packed, homogeneous OPA SAMs on titania films. Having established the formation of OPA SAMs on titania, we investigated their stability upon exposure to various liquids, UV light, air plasma and heat. For this purpose, only well-ordered monolayers prepared from 2×10^{-4} M OPA solution in THF were used.

3.2. Stability of OPA SAMs on titania films

3.2.1. Exposure to various solvents

The stability of OPA SAMs on amorphous titania films upon exposure to liquids with different dielectric constants was investigated. For this purpose, water, methanol, ethanol, acetone, cyclohexane and toluene were used. The stability of these SAMs on titania films was investigated by advancing water contact angle measurements (Table 1). An advancing water contact angle of 110 ± 2° was measured on OPA SAMs after preparation. The wettability altered after 18 h immersion in different liquids.

No changes in water wettability were observed after immersion of OPA SAMs in cyclohexane, toluene and, within experimental error, acetone. On the other hand, a decrease in water contact angle has been measured on surfaces exposed to ethanol, methanol and water. A difference as high as ∼35° in water wettability was caused by exposure of the OPA SAMs to water. These data were in contradiction with the experiments of Gawalt et al. [7], who reported that alkanephosphonic acid assembled on oxidised titanium foil was easily removed by a solvent rinse, unless heated. We found that no heat treatment was necessary to impart stability to OPA SAMs on titania films.

Our results suggest that the molecules of certain liquids can penetrate the pores of the adsorbed OPA monolayers, thus changing their conformation. Similar behaviour has been reported for other systems [30]. Since one would expect liquids with

Table 1
Changes in water wettability of OPA SAMs on titania after 18 h exposure to various liquids

Fluid	ε (25 °C)	Water contact angle before immersion	Water contact angle after 18 h immersion	$\Delta\theta$
Air (control experiment)	1.0	110.0 ± 2.0	111.8 ± 0.9	−1.8
Cyclohexane	2.0	111.0 ± 2.4	111.6 ± 0.4	−0.6
Toluene	2.4	110.0 ± 0.5	107.8 ± 1.4	2.2
Acetone	20.7	110.8 ± 0.9	108.2 ± 2.1	2.6
Ethanol	24.3	110.5 ± 1.9	100.6 ± 1.4	9.9
Methanol	32.6	108.9 ± 2.1	91.4 ± 1.3	17.5
Water	78.5	109.5 ± 2.1	75.1 ± 3.3	34.4

Experimental conditions for the deposition were 6 h immersion in a 2×10^{-4} M OPA in THF. Advancing water contact angles and standard deviations are shown.

larger molecules to be less able to penetrate and remain in the monolayer than those having smaller molecules, we plotted the difference in water contact angles on OPA SAM caused by the solvent exposure as a function of molecular volume of the tested liquids (Fig. 4).

A dependence of water wettability on solvent molecular volume is observed. Fig. 4 suggests that liquid penetration or retention occurs on OPA SAM adsorbed on titania films. Whereas smaller molecules (ethanol, methanol and water) penetrate into the solid film of OPA, large molecules are unable to do so. Our data show that molecules of solvents with molecular volume above 140 Å^3 are too large to penetrate the OPA films. This is illustrated by water contact angle data obtained on cyclohexane and toluene where no changes in water wettability were observed. Following Timmons and Zisman [31], an estimate of the average cross-sectional area of the intermolecular pores in the adsorbed OPA monolayer would be approx. 27 Å^2. This calculation is based on the assumption that the molecules of a liquid are spherical.

3.2.2. The influence of UV light

We investigated the influence of UV light irradiation on the stability of OPA SAM on titania films. Fig. 5 shows the advancing water contact angle as a function of UV light energy. It can be seen that water contact angle decreases with UV light irradiation. The surface turns into a completely hydrophilic state after a dose of approximately 4 J/cm^2 (approx. 60 min in our experiments).

Fig. 6 shows a high-resolution XPS carbon C(1s) peak acquired from the OPA SAMs on titania films as a function of UV light irradiation.

A decrease in the amount of carbon caused by UV light exposure can be seen. This is in accordance with water contact angle measurements and shows that a gradual decomposition of the hydrocarbon chain takes place. Normalized C(1s) spectra (Fig. 8) show that an initially symmetrical carbon C(1s) peak turns into an asymmetrical one following UV light exposure. The broadening on the high-energy side of the peak (at 286.6 eV, revealed by curve fitting procedure), accompanied by a shoulder centred at 288.8 eV can be observed in Fig. 6.

XPS spectra were also acquired from OPA SAMs on titania films after longer UV light exposure—90, 120 and 180 min (water contact angle was 0° in all cases). These spectra were virtually identical. This confirms that carbon-chain decomposition has taken place in the first 60 min, as shown in parallel by contact

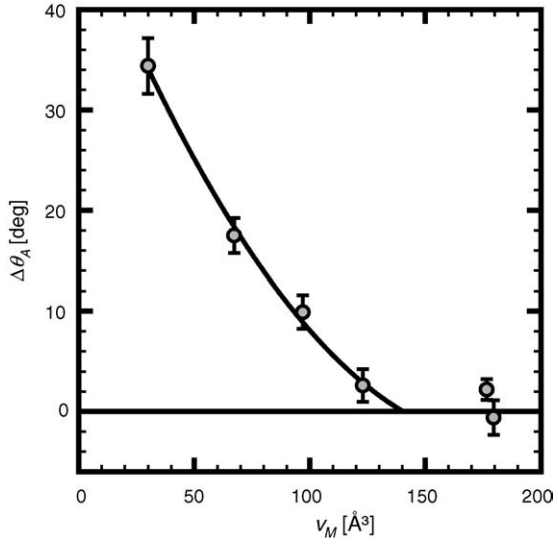

Fig. 4. Changes in the advancing contact angle of water on OPA SAMs (measured before and after 18 h immersion in different solvents) as a function of the molecular volume of the solvent.

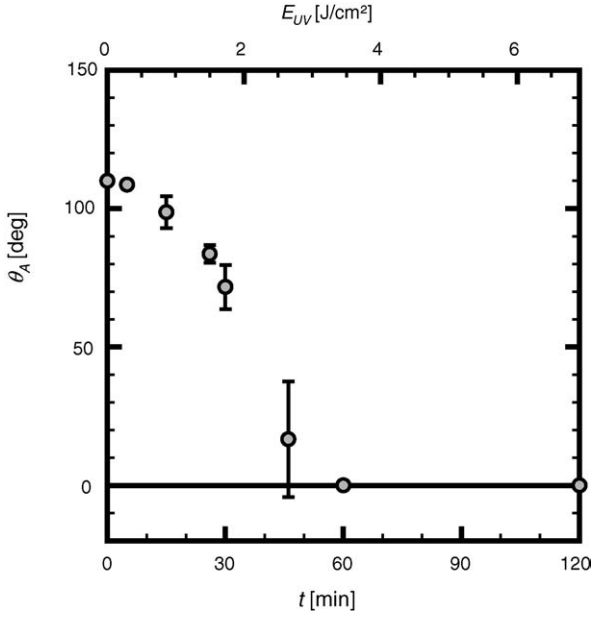

Fig. 5. Advancing contact angle of water on OPA SAMs formed on titania films as a function of time of exposure to UV light (λ = 250 nm, intensity 1 mW/cm^2).

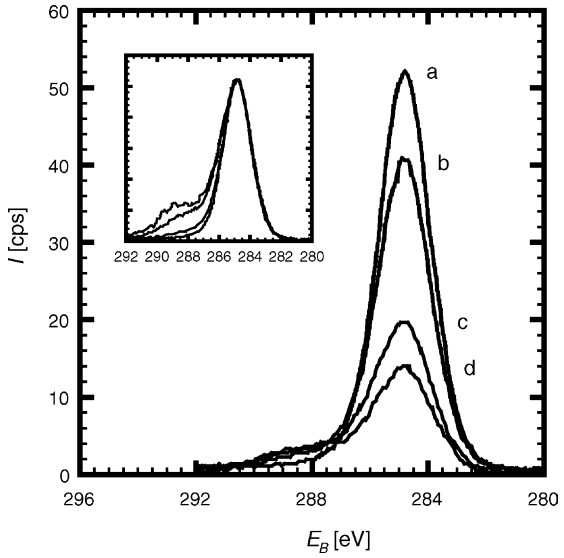

Fig. 6. High-resolution XPS spectrum of carbon C(1s) acquired from OPA SAMs formed on titania films after an exposure to UV light of (a) 0 min; (b) 15 min; (c) 45 min; and (d) 75 min. Inset: same spectra after normalization.

angle data. In order to obtain information on the hydrophilic surface, we paid particular attention to the presence of phosphorus atoms. The surface concentration of phosphorus (as determined by the XPS P(2p) photo-peak) is plotted in Fig. 7 as a function of UV light exposure. It can be seen that the amount of phosphorus is not significantly altered by further exposure to UV light.

These observations show that the carbon-chain of OPA SAMs on titania films is decomposed when exposed to UV light. The decomposition is caused by the photocatalytic properties of the underlying titania films. As a control experiment, we investigated the influence of OPA SAMs adsorbed on smooth alumina films. A water contact angle of 110° was measured on OPA

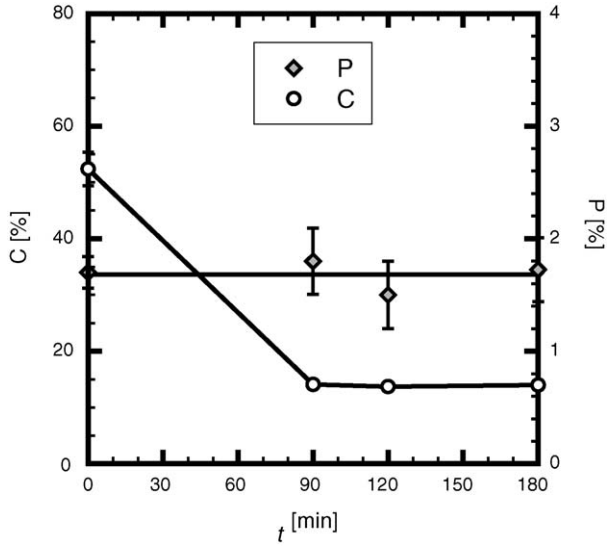

Fig. 7. The surface concentration of phosphorus and carbon on OPA SAMs formed on titania films after exposure to UV light as determined from the XPS P(2p) photo-peak.

SAMs on the surface of alumina both before and after UV light irradiation under identical experimental conditions, due to the absence of photocatalysis.

On the surface of titania, UV light generates reactive oxidising radicals, which abstract hydrogen atoms from the hydrocarbon chain [25]. The attack of oxidizing species produce alkoxy radicals and carbonyl species. These species are further decomposed via successive photocatalysis, forming shorter alkyl chains. This mechanism is similar to that discussed by Lee et al. [32] on alkylsiloxane SAMs on titania.

The presence of phosphorus atoms (Fig. 7) on the surface after long-exposure times illustrates that the phosphorus headgroups remain attached on the substrate even after the photodecomposition comes to a completion—only oxidation remnants (i.e. hydroxyl groups) are left on the surface.

3.2.3. The influence of air plasma

The influence of air plasma on the stability of OPA SAMs on titania has been investigated by contact angle measurements and XPS. It was found that air plasma significantly alters the structure of OPA SAMs on titania films—exposure to air plasma results in complete hydrophilicity. The water contact angle decreases to 0° in less that 1 s when exposed to air plasma. The XPS spectra (not shown) revealed the same trend as that caused by UV light—a decrease in the amount of carbon is caused by carbon chain shortening due to plasma etching and is accompanied by a broadening of the carbon peak (caused by oxidation of the carbon chain). Analogous to the influence of UV light, the damage and oxidation of the OPA SAMs due to plasma etching did not remove the phosphorus headgroup, which was revealed by the presence of phosphorus in the XPS spectra (after 1 min exposure).

3.2.4. The influence of exposure to ethanol, UV light and air plasma by ToF-SIMS

In order to independently verify the influence of external stimuli – exposure to solvent (ethanol), UV light and air plasma – TOF-SIMS spectroscopy was used. Table 2 summarizes three different treatments studied using TOF-SIMS.

The negative ion SIMS spectra of all three OPA SAMs studied exhibited the following dominant peaks: C^- (m/z 12.00), CH^- (m/z 13.01), CH_2^- (m/z 14.02), O^- (m/z 15.99), OH^- (m/z 17.00), C_2^- (m/z 24.00), C_2H^- (m/z 25.01), PO_2^- (m/z 62.96) and PO_3^- (m/z 78.97). The phosphorus P^- signal (m/z 30.97) was remarkably weak on all samples.

The intensities of the most dominant peaks in the mass range m/z = 0–200 acquired from the OPA SAMs attached onto titania

Table 2
Treatment of OPA SAMs on titania prior to ToF-SIMS analysis

	Surface treatment
I	Thorough rinse with Milli-Q water, sonication in ethanol for 10 min, followed by a rinse with copious amount of Milli-Q water. The samples were subsequently blown dry with filtered nitrogen.
II	Treatment (I) followed by UV light irradiation (250 nm, 9 J/cm^2)
III	Treatment (I) followed by exposure to air plasma for 60 s

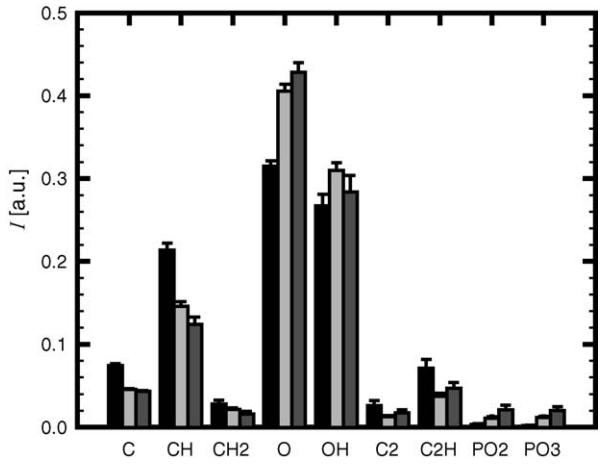

Fig. 8. Negative ToF-SIMS data acquired from OPA SAMs formed on titania films after various surface treatments. Black bar: water rinse and exposure to ethanol (treatment I); light grey bar: treatment I followed by exposure to UV light ($\lambda = 250$ nm, 9 J/cm^2); grey bar: treatment I followed by 60 s exposure to air plasma.

films after the treatments described in Table 2 are plotted in Fig. 8. The spectra were dominated by the same peaks after various treatments. The C_xH_y fragments do not provide specific structural information on the nature and structure the OPA SAMs, since they originate from both fragmentation of the OPA SAMs and from the naturally adsorbed hydrocarbons. Given the problems caused by adventitious hydrocarbon, we refrain here from lengthy speculation upon the origin of the peaks. We note, however, that the intensity of all carbon-containing species decreased following the exposure to UV light and air plasma. We ascribed this to the removal of the OPA carbon chain (as confirmed by the contact angle determination and the XPS). Water contact angle on samples exposed to ethanol (treatment I) was 110° whereas the samples exposed to UV light and air plasma were completely hydrophilic (0°).

Particular emphasis was placed upon the presence of phosphorus-containing species. The PO_3^- and PO_2^- signals were indicative of the OPA monolayer and were present on all samples. The presence of phosphorus-containing fragments (PO_2^-, PO_3^- and P^-) after exposure to these fragments following the exposure to UV light and air plasma corroborates the data obtained by the XPS and underlines the stability of the phosphate–titanium cation bond.

3.2.5. The influence of heat treatment

The influence of heat treatment in air on the stability of OPA SAMs on titania films was investigated by contact angle measurements and XPS. The decrease in the amount of carbon as assessed by the XPS matched wettability changes—water contact angle decreased to 0° following exposure to temperatures above 350 °C due to thermal decomposition of the alkyl chains. The effect of heat treatment is therefore, in terms of the OPA alkyl chain stability, similar to that caused by UV light and air plasma. We also investigated the stability of the phosphate–titanium bond exposed to high temperatures in air and found that phosphorus was present on the surface after heat treatment at temperatures as high 800 °C, but disappeared after heating at temperatures around 1000 °C.

4. Conclusion

Self-assembled monolayers of octadecylphosphonic acid can be deposited onto amorphous TiO_2 by immersion in OPA/THF solution. The formation of OPA SAMs is concentration dependent. The titania substrate is covered quickly by OPA self-assembled monolayers after immersion in 2×10^{-4} M OPA solution. Water wettability (110°) strongly suggests that well-ordered homogeneous OPA layers are present. The amorphous titania film is virtually instantly covered by a uniform monolayer of OPA. At lower concentrations (2×10^{-6} and 2×10^{-8} M OPA), only partial coverage of OPA on titania films is achieved.

The exposure of the closely-packed OPA SAMs to liquids of different dielectric constants shows that changes in water wettability are a function of molecular volume of the liquids. This is explained in terms of liquid penetration—low molecular volume liquids penetrate the OPA films, but no such behaviour occur after exposure of OPA SAMs to high molecular volume liquids. This points at a pores cross-sectional area of 27 Å^2.

UV light irradiation causes decomposition of the OPA SAMs due to photocatalytic properties of the underlying titania film. Intensive heat treatment causes decomposition of the alkyl chain of OPA SAMs. The exposure of OPA SAMs to air plasma causes etching of the carbon chain. UV light irradiation, heat treatment and exposure to air plasma significantly alter wettability of OPA SAMs, resulting in a water contact angle of 0°. The presence of phosphorus in the XPS and SIMS spectra obtained on these hydrophilic surfaces shows that the bond of the phosphate headgroup to the TiO_2 substrate through oxygen atom(s) is strong and can withstand the influence of these stimuli.

Acknowledgements

Financial support for this project from the Australian Research Council through the Special Research Centre Scheme is gratefully acknowledged. We thank Dr. Craig Priest for the preparation of OPA molecules and Mr. Marek Jasieniak for his assistance with the ToF-SIMS analysis.

References

[1] A. Ulman, An Introduction to Ultrathin Organic Films, Academic Press, 1991.
[2] G.J. Kluth, M.M. Sung, R. Maboudian, Thermal behavior of alkylsiloxane self-assembled monolayers on the oxidised Si(1 0 0) surface, Langmuir 13 (1997) 3775.
[3] N.J. Brewer, et al., Oxidation of self-assembled monolayers by UV light with a wavelength of 254 nm, J. Am. Chem. Soc. 123 (2001) 4089.
[4] Y.T. Tao, et al., Infrared and atomic force microscopy imaging study of the reorganization of self-assembled monolayers of carboxylic acids on silver surface, Langmuir 18 (2002) 8400.
[5] M. Textor, et al., Structural chemistry of self-assembled monolayers of octadecylphosphoric acid on tantalum oxide surfaces, Langmuir 16 (2000) 3257.

[6] E.S. Gawalt, et al., Enhanced bonding of alkanephosphonic acids to oxidized titanium using surface-bound alkoxyzirconium complex interfaces, Langmuir 15 (1999) 8929.
[7] E.S. Gawalt, et al., Self-assembly and bonding of alkanephosphonic acids on the native oxide surface of titanium, Langmuir 17 (2001) 5736.
[8] W. Gao, et al., Self-assembled monolayers of alkylphosphonic acids on metal oxides, Langmuir 12 (1996) 6429.
[9] R. Helmy, A.Y. Fadeev, Self-assembled monolayers supported on TiO_2: comparison of $C_{18}H_{37}SiX_3$ (X = H, Cl, OCH_3), $C_{18}H_{37}Si(CH_3)_2Cl$, and $C_{18}H_{37}PO(OH)_2$, Langmuir 18 (2002) 8924.
[10] I. Doudevski, W.A. Hayes, D.K. Schwartz, Submonolayer island nucleation and growth kinetics during self-assembled monolayer formation, Phys. Rev. Lett. 81 (22) (1998) 4927–4930.
[11] I. Doudevski, D.K. Schwartz, Dynamic scaling of the submonolayer island size distribution during self-assembled monolayer growth, Phys. Rev. B 60 (1) (1999) 14–17.
[12] I. Doudevski, D.K. Schwartz, Concentration dependence of self-assembled monolayer island nucleation and growth, J. Am. Chem. Soc. 123 (28) (2001) 6867–6872.
[13] I. Doudevski, D.K. Schwartz, Self-assembled monolayers in the context of epitaxial film growth, Appl. Surf. Sci. 175–176 (2001) 17–26.
[14] J.T. Woodward, D.K. Schwartz, In situ observation of self-assembled monolayer growth, Journal of the American Chemical Society 118 (33) (1996) 7861–7862.
[15] I. Doudevski, D.K. Schwartz, Concentration dependence of self-assembled monolayer island nucleation and growth, J. Am. Chem. Soc. 123 (2001) 6867.
[16] J.T. Woodward, A. Ulman, D.K. Schwartz, Self-assembled monolayer growth of octadecylphosphonic acid on mica, Langmuir 12 (1996) 3626.
[17] R.F. Gould, Contact Angle: Wettability and Adhesion, American Chemical Society, Washington, 1964.
[18] J.G. Van Alsten, Self-assembled monolayers on engineering metals: structure, derivatization, and utility, Langmuir 15 (1999) 7605.
[19] R. Hofer, M. Textor, N.D. Spencer, Alkyl phosphate monolayers, self-assembled from aqueous solution onto metal oxide surfaces, Langmuir 17 (2001) 4014.
[20] D. Brovelli, et al., Highly oriented, self-assembled alkanephosphate monolayers on tantalum(V) oxide surfaces, Langmuir 15 (1999) 4324.
[21] M. Bjelopavlic, J. Ralston, G. Reynolds, Adsorption of monoalkyl phosphates at the zircon-aqueous solution interface, J. Colloid Interface Sci. 208 (1998) 183.
[22] N. Pelaprat, et al., Synthèse D'Alkylphosphonates À Longues Chaines Hydrocarbonèes, Modifications Chemiques et Applications. II. Addition de HP(O)(OEt)2 Sur Les Alcènes et Phosphonation Directe D'Halogènures D'Alkyles, Eur. Polym. J. 32 (1996) 761.
[23] G. Solomons, C. Fryhle, Organic Chemistry, seventh ed., John Wiley and Sons, 2000.
[24] A. Feiler, P. Jenkins, J. Ralston, Metal oxide surfaces separated by aqueous solutions of linear polyphosphates; DLVO and non-DLVO interaction forces, Phys. Chem. Chem. Phys. 2 (2000) 5678.
[25] A. Kanta, R. Sedev, J. Ralston, Thermally- and photo-induced changes in the water wettability of low-surface-area silica and titania, Langmuir 21 (2005) 2400.
[26] E. Cooper, G.J. Leggett, Static secondary ion mass spectrometry studies of self-assembled monolayers: influence of adsorbate chain length and terminal functional group on rates of photooxidation of alkanethiols on gold, Langmuir 14 (1998) 4795.
[27] I. Doudevski, W.A. Hayes, D.K. Schwartz, Submonolayer island nucleation and growth kinetics during self-assembled monolayer formation, Phys. Rev. Lett. 81 (1998) 4927.
[28] J.T. Woodward, D.K. Schwartz, In situ observation of self-assembled monolayer growth, J. Am. Chem. Soc. 118 (1996) 7861.
[29] C. Messerschmidt, D.K. Schwartz, Growth mechanism of octadecylphosphonic acid self-assembled monolayers on sapphire (corundum); evidence for a quasi-equilibrium triple point, Langmuir 17 (2001) 462.
[30] C.N.C. Lam, et al., The effect of liquid properties to contact angle hysteresis, Colloids Surf. A: Physicochem. Eng. Aspects 189 (2001) 265.
[31] C.O. Timmons, W.A. Zisman, The effect of liquid structure on contact angle hysteresis, J. Colloid Interface Sci. 22 (1966) 165.
[32] J.P. Lee, et al., Photocatalytic decomposition of alkylsiloxane self-assembled monolayers on titanium oxide surfaces, J. Phys. Chem. 107 (2003) 8997.